Article

Not peer-reviewed version

Interplay Between Immune Checkpoint Modulators and the Epithelial-to-Mesenchymal Transition Axis in Clear Cell Renal Cell Carcinoma

Arpita Poddar [†], Farah Ahmady-Nield [†], Revati Sharma, Seemadri Subhadarshini, Mohit Kumar Jolly, Suresh Ramakrishna, Ali Raza, Ravi Shukla, George Kannourakis, Aparna Jayachandran [*], Prashanth Prithviraj [*]

Posted Date: 30 April 2026

doi: 10.20944/preprints202604.2137.v1

Keywords: immune checkpoint inhibitors; epithelial-to-mesenchymal transition; clear cell renal cell carcinoma; LAG3; NT5E; PD-L1; survival; biomarkers; single cell RNA sequencing; AUC

Article

Interplay Between Immune Checkpoint Modulators and the Epithelial-to-Mesenchymal Transition Axis in Clear Cell Renal Cell Carcinoma

Arpita Poddar [1,2,3,4,†], Farah Ahmady-Nield [1,2,†], Revati Sharma [1], Seemadri Subhadarshini [5,6], Mohit Kumar Jolly [5], Suresh Ramakrishna [7,8], Ali Raza [1], Ravi Shukla [3,9,10], George Kannourakis [1,2], Aparna Jayachandran [1,2,*] and Prashanth Prithviraj [1,2,*]

[1] Fiona Elsey Cancer Research Institute, Ballarat, Victoria 3350, Australia
[2] School of Institute of Innovation, Science and Sustainability, Federation University, Ballarat, Victoria 3350, Australia
[3] Ian Potter NanoBiosensing Facility, NanoBiotechnology Research Laboratory, School of Science, RMIT University, Melbourne, Victoria 3000, Australia
[4] Department of Surgery, The Royal Melbourne Hospital, The University of Melbourne, Parkville, Victoria 3050, Australia
[5] Department of Bioengineering, Indian Institute of Science, Bengaluru, Karnataka 560012, India
[6] Nuffield Department of Medicine, University of Oxford, Oxford, OX3 7BN, United Kingdom
[7] Graduate School of Biomedical Science and Engineering, Hanyang University, Seoul, 04763, South Korea
[8] College of Medicine, Hanyang University, Seoul, 04763, South Korea
[9] Centre for Advanced Materials and Industrial Chemistry, RMIT University, Melbourne, VIC 3001, Australia
[10] School of Health & Biomedical Science, RMIT University, Melbourne, Victoria 3000, Australia
* Correspondence: aparna@fecri.org.au (A.J.); prashanth@fecri.org.au (P.P.)
† These authors contributed equally to this work.

Simple Summary

Clear cell renal cell carcinoma (ccRCC) is the most common and most aggressive form of kidney cancer. While some patients benefit from immune checkpoint inhibitor therapies, overall outcomes remain poor for many. Research has mainly focused on PD-1 and PD-L1, whereas the role of other immune checkpoint molecules and their relationship with epithelial-to-mesenchymal transition (EMT), a process associated with tumor progression, immune escape and metastasis, remains less well understood. In this study, we found that several immune checkpoints were altered in ccRCC tumors, particularly LAG3 and NT5E, and that higher expression of these genes was associated with poorer survival. Importantly, combining immune checkpoint and EMT markers provided better prognostic information than immune checkpoint markers alone. These findings suggest that an EMT–immune checkpoint axis involving LAG3 and NT5E may contribute to ccRCC progression and help identify patients with more aggressive disease, supporting future risk stratification and therapeutic strategies.

Abstract

Background/Objectives: Clear cell renal cell carcinoma (ccRCC), the predominant malignant subtype of kidney cancer, is the leading cause of death among renal cell carcinoma patients. Although a subset of ccRCC patients benefit from select immune checkpoint inhibitors (ICIs), prognosis remains poor. While PD-1 and PD-L1 have been extensively studied, the prevalence and distribution of other immune checkpoints (ICs) and their relationship with epithelial-to-mesenchymal transition (EMT) remain poorly characterized. Here, we investigated the interplay between twenty ICs and EMT markers and assessed their combined prognostic relevance in ccRCC patients. **Methods**: Transcriptomic profiling and integrated bioinformatic analyses were performed, including differential expression, correlation analyses, survival analyses, forest plot analyses, ROC curve

 doi:10.20944/preprints202604.2137.v1

evaluation, and OncoPrint visualisation, complemented by analysis of single-cell RNA sequencing data, immunohistochemistry, and multiplex secretory IC (LegendPlex) assays. **Results**: Transcriptomic profiling of over 500 ccRCC tumors versus normal kidney tissue revealed dysregulation of ICs, particularly LAG3 and NT5E. Notably, expression of ICs, including LAG3 and NT5E, was associated with poor overall survival in 415 ccRCC patients. ICs that synergised with EMT phenotype provided improved prognostic discrimination compared to individual ICs. Correlation analyses, single-cell RNA sequencing and immunohistochemistry demonstrated that EMT-associated tumor cells exhibit coordinated expression of LAG3 and NT5E. Receiver operating characteristic analysis highlighted the potential clinical utility of LAG3 and NT5E. **Conclusions**: Collectively, this study defines an EMT-IC axis in ccRCC and demonstrates its relevance to tumor biology and patient outcomes, highlighting LAG3 and NT5E as potential prognostic markers and therapeutic targets.

Keywords: immune checkpoint inhibitors; epithelial-to-mesenchymal transition; clear cell renal cell carcinoma; LAG3; NT5E; PD-L1; survival; biomarkers; single cell RNA sequencing; AUC

1. Introduction

Renal cell carcinoma (RCC) is one of the most common genitourinary tumors. RCC constitutes a diverse group of malignancies arising from the nephric epithelial cells and affects nearly 400,000 individuals worldwide each year [1]. Clear cell RCC (ccRCC) represents the most frequent and best-studied RCC histological subtype characterised by the clear cytoplasm in cells. ccRCC accounts for approximately 80% of all RCC cases and contributes to over 175,000 deaths each year [2,3]. When diagnosed early, ccRCC patients can be successfully treated with surgical or ablative strategies. However, up to a third of ccRCC patients present with metastases, and a third of ccRCC patients develop metastases during follow up [4]. The 5-year survival rate of ccRCC patients is 50%, while metastatic RCC patients have a 5-year survival rate of 5-10% after diagnosis [5,6]. ccRCC is typically non-responsive to traditional chemotherapeutic drugs and radiation therapy [7]. Considering the pathogenetic role of the Von Hippel Lindau (VHL) protein in ccRCC and the highly vascular nature of this RCC subtype, anti-angiogenic strategies with small-molecule tyrosine kinase inhibitors (TKI) have become a promising therapeutic approach for the treatment of ccRCC [8]. The following TKI small-molecule inhibitor drugs primarily targeting the vascular endothelial growth factor (VEGF) signalling pathway have been approved for clinical use: sunitinib, sorafenib, axitinib, cabozantinib, lenvatinib and pazopanib [9]. Mammalian target of rapamycin (mTOR) inhibitor drugs everolimus and temsirolimus have been approved for ccRCC patient treatment [10].

More recently, immunotherapy in the form of immune checkpoint inhibition has dramatically changed the standard of care for ccRCC patients [2]. Within the tumor microenvironment (TME), the immune checkpoint (IC) interactions are often dysregulated leading to suppressed T-cell effector functions. Immune checkpoint inhibitors (ICIs) effectively targeting these checkpoint molecules can re-animate the tumor-specific T-cell immunity, leading to more durable responses than TKI therapy alone [2,11]. Treatment with ICIs has been effective as ccRCC is an immunogenic tumor with high numbers of immune cells [2,12–14]. The best characterised ICIs targeting Programmed cell-Death 1 (PD-1), Programmed Death Ligand 1 (PD-L1) and Cytotoxic T-lymphocyte-associated antigen 4 (CTLA4) have been shown to reduce the immune escape of cancer cells and suppress tumor growth. Nivolumab or Pembrolizumab (anti-PD-1 blockers) and Avelumab (anti-PD-L1 blocker) used as monotherapy or as a combination with Ipilimumab (anti-CTLA4 blocker) or anti-angiogenic drugs in both first- and second-line treatment settings in ccRCC have shown efficacy and overall survival benefits [15,16].

Despite the substantial clinical response of ICIs, their efficacy is generally limited to a subset of cancer patients. To date, ICI monotherapies achieve only a modest overall response rate (ORR) of 21–36% [2]. Combination regimens, including dual ICI blockade or ICI–TKI combinations have improved ORR of 34–73%; nevertheless, many patients still do not achieve lasting responses, and

 doi:10.20944/preprints202604.2137.v1

those who are unresponsive to ICI-based treatments continue to experience poor clinical outcomes [17,18]. Furthermore, high grade 3 or 4 ICI-related adverse events occur in a significant proportion of patients [16]. Anti-tumor responses to ICI therapy vary between cancer types and even among patients with the same histological subtype [19,20]. Tumors initially responsive to ICI therapy eventually progress during treatment due to acquired resistance [21]. PD-L1 expression alone is insufficient as a predictive biomarker in ccRCC [22]. Consequently, there is an urgent need to identify additional prognostic and predictive biomarkers to guide patient selection. Alternative IC pathways may reveal novel biomarkers and therapeutic targets, enabling rational combination strategies that synergise with PD-1 and/or CTLA-4 axes blockade to enhance clinical efficacy in ccRCC.

The cellular reprogramming process called epithelial-to-mesenchymal transition (EMT) is a form of cellular plasticity that underlies ICI resistance and promotes relapse, metastases and unfavourable patient outcomes [23,24]. EMT is a multistep biological process facilitating the switching of cellular phenotypes. During this process, epithelial cells acquire mesenchymal phenotype and function [25]. The process of EMT leading to cancer initiation, progression and acquisition of drug resistance has been implicated in immune evasion of cancer cells across several malignancies, including ccRCC [19,20,24,26]. Emerging evidence links EMT status with altered expression of IC molecules in ccRCC patients [27,28], suggesting that cellular plasticity within the heterogeneous TME directly shapes anti-tumor immune responses.

This study aimed to investigate the interplay between EMT and IC expression in ccRCC, to define an EMT-IC axis, assess its prognostic relevance, and identify key ICs with potential as biomarkers and therapeutic targets. We compared the expression of IC molecules in healthy kidney and ccRCC tumor samples and analysed a panel of twenty ICs and EMT-associated genes using datasets from SurvExpress and GEO. Prognostic significance was evaluated using survival analyses, forest plots, and receiver operating characteristic curves. LegendPlex assays were performed to assess changes in secretory ICs before and after ICI treatment in a ccRCC patient. Correlation analyses, single-cell RNA sequencing, and immunohistochemistry were utilised to examine co-expression and spatial association of EMT-like tumour cells with key ICs, particularly NT5E and LAG3. Collectively, these analyses define an EMT–IC axis, linking EMT phenotype with IC highlight NT5E and LAG3 as promising prognostic markers and therapeutic targets in ccRCC.

2. Materials and Methods

2.1. OncoPrint Analysis of Immune Checkpoints Using cBioPortal

OncoPrint from cBioPortal (http://cbioportal.org) was used to obtain a compact graphical summary of gene expression alterations in IC genes across 537 ccRCC patient samples. Within cBioPortal, we utilised the Kidney Renal Clear Cell Carcinoma (TCGA, GDC) case set to study gene alterations in IC genes. ccRCC patients are represented as columns, and IC genes are represented as rows. Genomic alterations, including amplifications and deletions, alterations in gene expressions and mutations are summarised by glyphs and colour coding. All cases are arranged as per alterations [29].

2.2. Bulk RNA-seq Data

RNA-sequencing transcriptomic data for 538 ccRCC tumors and 72 adjacent normal kidney tissue samples were obtained from the TCGA Kidney Renal Clear Cell Carcinoma (KIRC) STAR-aligned TPM dataset hosted by UCSC Xena (https://xenabrowser.net) [30]. Gene expression values were quantified as transcripts per million (TPM) and were log2-transformed [log2(TPM + 1)] prior to downstream analyses. Differential gene expressions between normal kidney and ccRCC tumor samples was performed using GraphPad Prism.

 doi:10.20944/preprints202604.2137.v1

2.3. Prognostic Analysis

Cox proportional hazards regression analyses were performed using the SurvExpress online tool to evaluate the prognostic impact of immune checkpoint and EMT gene expression in 415 ccRCC patients (http://bioinformatica.mty.itesm.mx:8080/Biomatec/SurvivaX.jsp) [31]. For SurvExpress analyses, duplicated genes were averaged across all probe-sets to generate a single expression value per sample, and the original quantile-normalised database was used. Kaplan–Meier survival curves, hazard ratios, and 95% confidence intervals were calculated in RStudio to visualise survival differences and validate the prognostic effect of individual genes or combined gene signatures. Forest plots were generated in RStudio to visualise the prognostic impact of individual immune checkpoints or combined EMT–IC gene signatures. Receiver operating characteristic (ROC) curves were also generated in SurvExpress to assess the discriminative performance of individual immune checkpoints and combined EMT–IC signatures for predicting overall survival. ROC curves were calculated by ranking patients based on gene expression–derived risk scores from Cox models, and sensitivity and specificity were assessed across these rankings. Area under the curve (AUC) values with 95% confidence intervals quantified prognostic accuracy.

2.4. Single-cell RNA Sequencing (scRNA-seq) Data

Publicly available count matrices for single-cell transcriptomic data from seven ccRCC patients were obtained from GEO (GSE210038). Activity scores for pathways and gene lists were computed on the gene expression values using AUCell [32]. The ccRCC.epi and ccRCC.mes signatures were applied to classify epithelial and mesenchymal tumor cells, respectively [33].

2.5. Correlation Analysis

Correlation analyses between EMT marker and IC genes were performed using bulk RNA-seq data from 535 ccRCC patients obtained from TCGA (GDC) via cBioPortal. Gene expression values were combined and normalised as FPKM Z-scores. Pearson and Spearman correlation coefficients were calculated in RStudio, and correlation tables were generated to assess the relationships between EMT and IC genes.

2.6. Immunohistochemistry Analysis

Immunohistochemistry was performed to assess colocalisation of LAG3 or NT5E with N-Cad or E-Cad using previously established protocols [34]. Paraffin-embedded tissue sections were deparaffinised, rehydrated, and subjected to antigen retrieval (pH 9.0 for N-Cad/E-Cad). Endogenous peroxidase activity was quenched with Dako peroxidase blocking solution, and non-specific binding was blocked with goat casein. Primary N-Cad antibody (Abcam ab98952; 1:1500) or E-Cad antibody (Cell Signalling Technology mAb 4A2; 1:100) was applied overnight at 4°C, followed by Dako Rabbit/Mouse secondary antibody (ENV K5007) and TSATM-GFP (1:100) labelling. Slides were then reprocessed for antigen retrieval (pH 9.0 for LAG3; pH 6.0 for NT5E), followed by peroxidase and non-specific protein blocking. Sections were incubated overnight at 4°C with NT5E (Cell Signalling Technology mAb #13160; 1:100) or LAG3 (Abcam ab209236; 1:10) antibodies, followed by secondary antibody incubation and TSATM-Cy5 (1:100) detection. Nuclei were counterstained with DAPI, and slides were mounted using ProLong® Diamond antifade mountant. Imaging was performed using an EVOS™ FL Auto 2 system.

2.7. Multiplex Quantification of Soluble Immune Checkpoint Proteins

Plasma levels of soluble IC proteins were quantified using the LEGENDplex™ Human Immune Checkpoint Panel 1 (10-plex), according to the manufacturer's instructions (Revvity, Australia). This bead-based multiplex immunoassay enables simultaneous detection of multiple analytes using flow cytometry. Briefly, patient plasma samples were incubated with fluorescently labelled capture beads conjugated to antibodies specific to IC proteins. Following incubation with detection antibodies and

 doi:10.20944/preprints202604.2137.v1

streptavidin-phycoerythrin, samples were acquired on a flow cytometer. Data were analysed using LEGENDplex™ software to determine analyte concentrations based on standard curves.

2.8. Statistical Analysis

All statistical analyses were performed in GraphPad Prism (GraphPad 10.2.3 Software) and R (version 4.3.1) using RStudio (version 2025.9.2.418). Differences in gene expression between normal kidney tissue and ccRCC tumors were assessed using the Wilcoxon rank-sum test. A p-value < 0.05 was considered statistically significant. RStudio was used to compute Kaplan–Meier analyses, hazard ratios (HRs) and 95% confidence intervals from Cox proportional hazards regression models. The concordance index (C-index) was computed to assess predictive performance. ROC curves were generated in SurvExpress to evaluate the discriminative ability of individual ICs and combined EMT–IC signatures, with area under the curve (AUC) values calculated to quantify prognostic accuracy. Forest plots depicting HRs were generated in RStudio. Pearson and Spearman correlation analyses were also performed in RStudio to assess relationships between EMT and IC genes. Statistical significance across all analyses was represented consistently as: $p < 0.05$ (*), $p < 0.01$ (**), and $p < 0.001$ (***). All tests were two-sided, and p-values < 0.05 were considered statistically significant.

3. Results

3.1. Dysregulation of IC molecules in ccRCC patients

To identify IC molecules linked with immune escape in ccRCC, we analysed a panel of 20 genes based on our previous studies demonstrating associations between immune-modulatory genes and overall survival and recurrence in other solid cancers [19,20]. This panel comprised both immune stimulatory and inhibitory genes including, Hepatitis A Virus Cellular Receptor 2 (HAVCR2 (TIM-3)), Cluster of Differentiation 28 (CD28), Tumor Necrosis Factor Receptor Superfamily Member 9 (TNFRSF9 (CD137)), Fas Ligand (FASLG (CD95L)), T cell immunoreceptor with Ig and ITIM domains (TIGIT), Galectin-9 (LGALS9), Cluster of Differentiation 80 (CD80), Cluster of Differentiation 27 (CD27), CTLA4, Lymphocyte Activation Gene-3 (LAG3), Indoleamine 2,3-dioxygenase 1 (IDO-1), V-Set Immunoregulatory Receptor (VSIR), PDCD1 (PD-1), Cluster of Differentiation 276 (CD276 (B7-H3)), Ecto-5′-Nucleotidase (NT5E (CD73)), Tumor Necrosis Factor Receptor Superfamily Member 14 (TNFRSF14 (HVEM)), B- and T-Lymphocyte Attenuator (BTLA), PD-L1 (CD274), VTCN1 (B7-H4) and Tumor Necrosis Factor Receptor Superfamily Member 18 (TNFRSF18 (GITR)).

Differential expression of IC genes was evaluated using RNA-seq data from 538 ccRCC tumors and 72 adjacent normal kidney tissue samples obtained from the TCGA KIRC dataset. Comparative analysis revealed that the majority of IC genes analysed were significantly upregulated in ccRCC tissues relative to normal kidney tissues (***$p < 0.001$), suggesting the presence of an immunosuppressive tumor microenvironment (Figure 1). Next, the expression profiles and genetic alterations of these 20 IC molecules in ccRCC patient tumors (n = 537) were assessed using OncoPrint analysis from cBioPortal. OncoPrint analysis revealed heterogeneous patterns of amplification, deletion, and mutation in several IC genes across the cohort (Supplementary Figure S1).

 doi:10.20944/preprints202604.2137.v1

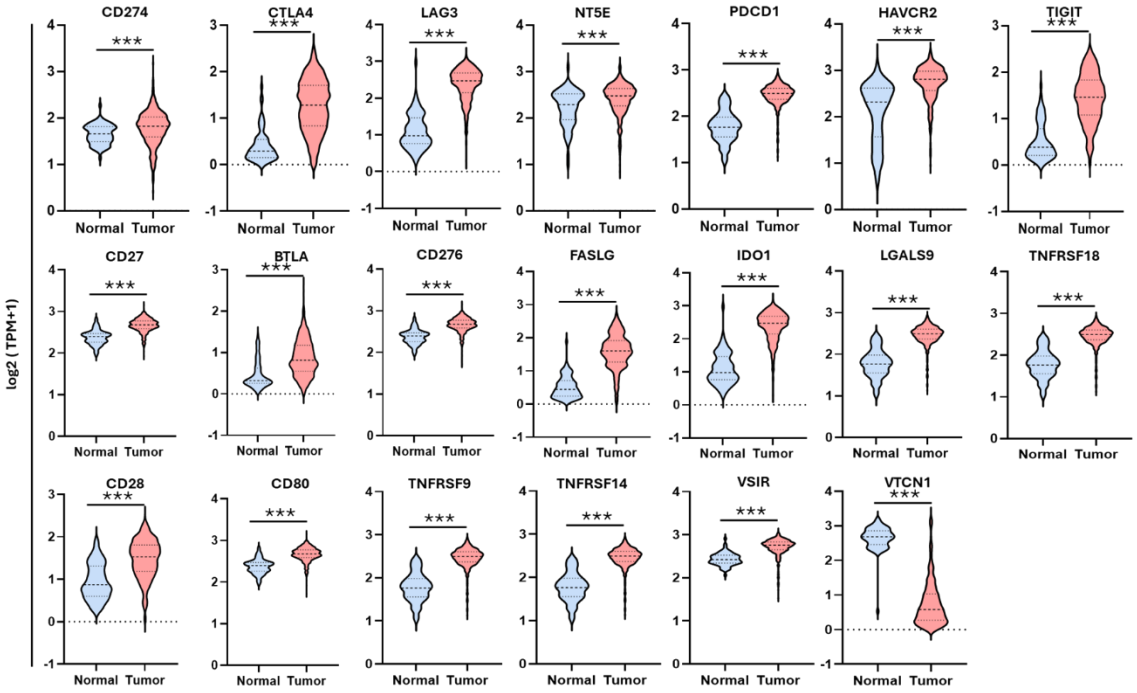

Figure 1. Violin plots illustrate the relative expression of 20 IC molecules in adjacent normal kidney tissue samples (blue) and ccRCC tumors (red). Gene expression values were log2-transformed [log2(TPM + 1)]. Statistical significance was assessed using the Wilcoxon rank-sum test. ***$p < 0.001$.

A bead-based multiplex LegendPlex immunoassay was performed to explore modulation of IC proteins following immunotherapy with Nivolumab. Plasma samples collected pre and post Nivolumab treatment from a ccRCC patient were analysed. This patient had progressive disease, deterioration in general condition and subsequently passed away. In plasma collected two-week post-treatment, analysis demonstrated a demonstrated a reduction in soluble PD-L1 levels, accompanied by increased levels of multiple IC proteins, including PD-1, CTLA4, LAG3, Galectin-9 (LGALS9), TIM-3, CD27, CD25 and 4-1BB, indicating systemic immune modulation following PD-1 blockade (Supplementary Figure S2). Overall, the observed dysregulation of multiple IC molecules in ccRCC highlights the potential utility of immunotherapeutic strategies targeting alternative or compensatory immune checkpoints in this cancer subtype.

3.2. ICs prognosticate Poor Survival in ccRCC Patients

To investigate the prognostic relevance of IC genes in ccRCC, we evaluated overall survival in a cohort of 415 ccRCC patient using SurvExpress. Kaplan-Meier survival risk curves for individual immune modulators were generated. Notably, altered expressions of CD80, CTLA4, TNFRSF18, LAG3, CD275, LGALS9, CD27, NT5E and TIGIT were associated with significantly reduced overall survival (Figure 2). In contrast, expression levels of other IC genes showed no significant correlation with overall survival (Supplementary Table S1). This finding suggests that individual ICs may contribute differently to patient outcomes, supporting their consideration as potential therapeutic biomarkers and targets.

 doi:10.20944/preprints202604.2137.v1

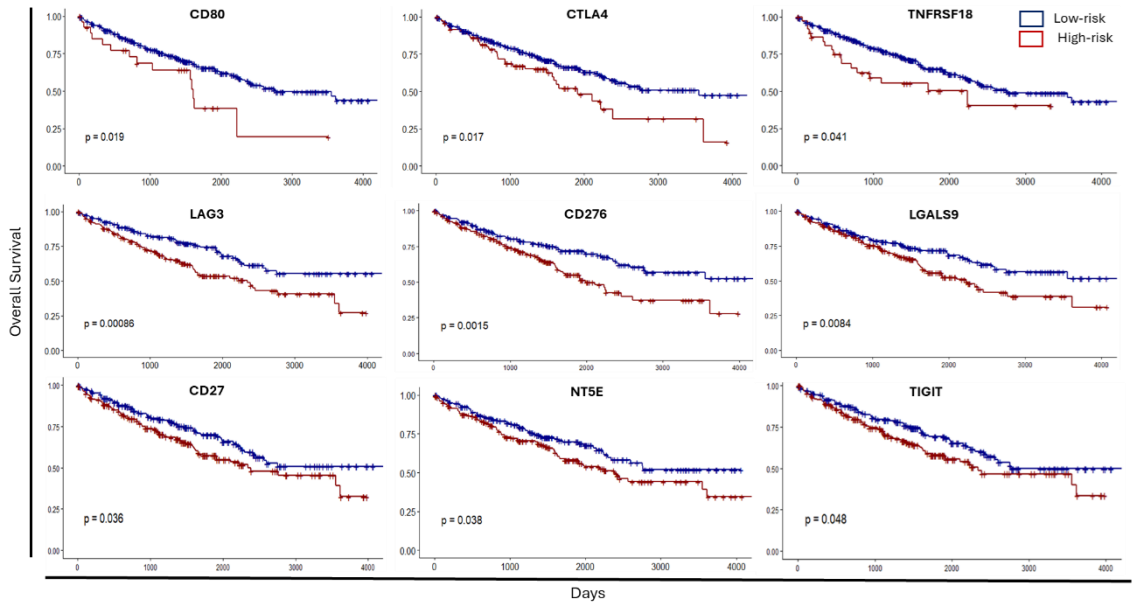

Figure 2. Association between immune modulators and overall survival in ccRCC patients. Kaplan–Meier survival curves generated for the analysis of survival and gene expression of CD80, CTLA4, TNFRSF18, LAG3, CD276, LGALS9, CD27, NT5E and TIGIT in 415 ccRCC patients. Blue curve represents low-risk group, while red curve represents high-risk group. The study time (days) is presented in the x-axis.

3.3. Association of IC Genes with EMT Markers Supports an EMT–IC Axis in ccRCC

To evaluate the prognostic significance of IC genes, Cox proportional hazards analysis was performed and visualised using forest plots. Among the 20 IC genes analysed, only a subset (n = 9) demonstrated a statistically significant association with overall survival in ccRCC patients (Figure 3A).Given the emerging role of EMT in regulating tumor immune evasion and IC expression, we evaluated the coordinated relationship between EMT markers and IC molecules to explore a potential EMT–IC axis in the same 415 ccRCC patient cohort. EMT markers E-Cadherin (CDH1), N-Cadherin (CDH2), Snail (SNAI1), Slug (SNAI2), Twist1 and Zeb1 were selected, as they represent key components of the EMT program, including loss of epithelial characteristics and activation of mesenchymal and transcriptional drivers of EMT. Notably, when combined with EMT gene expression, all IC genes exhibited a significant association with overall survival (Figure 3B). Furthermore, hazard ratios (HRs) for individual IC genes were generally modest (HR < 2). However, when analysed in combination with EMT markers, HR values increased substantially, with all genes exhibiting HRs greater than 2, indicating an enhanced prognostic effect.

To further identify IC genes strongly associated with the EMT phenotype in ccRCC, correlation analyses were performed in 535 patients between 20 ICs and 6 EMT-related genes. Pearson correlation analysis revealed that most ICs and EMT-related genes were negatively correlated with CDH1, consistent with EMT activation, while correlations with CDH2 were generally weaker. LAG3 showed a robust positive correlation with TWIST1, CD276 correlated strongly with TWIST1 and SLUG and modestly with SNAIL, and NT5E showed a modest correlation with SLUG. (Figure 4A).

 doi:10.20944/preprints202604.2137.v1

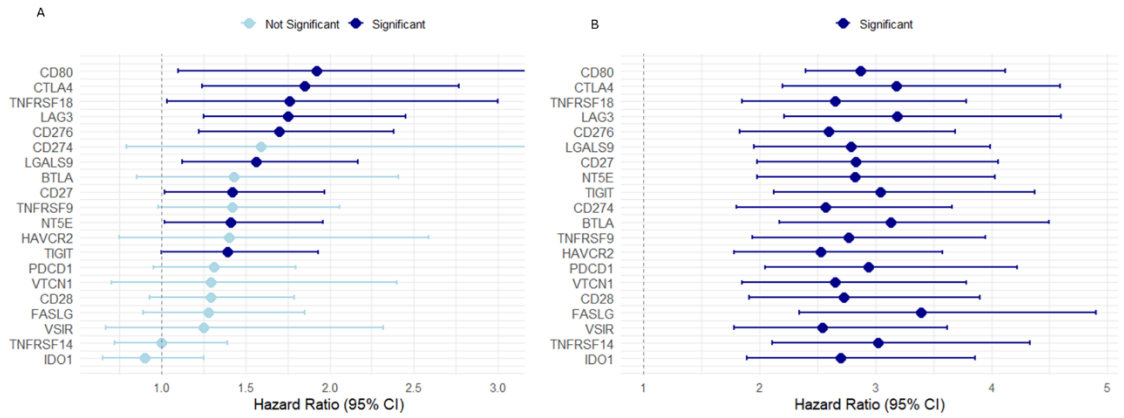

Figure 3. Prognostic impact of IC genes alone and in combination with EMT markers in ccRCC patients. Forest plot showing Cox proportional hazards analysis of (A) 20 IC genes individually and (B) IC genes analysed in combination with EMT markers. Genes with statistically significant association with overall survival are highlighted in dark blue, while non-significant genes are shown in light blue. Hazard ratios and 95% confidence intervals are shown.

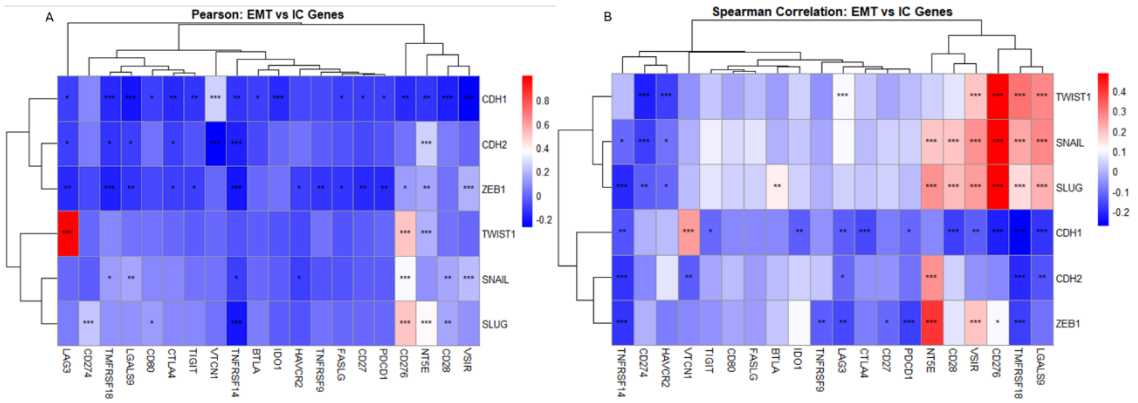

Figure 4. Correlation analysis of IC genes and EMT markers in ccRCC. (A) Pearson and (B) Spearman correlation analyses were performed in 535 ccRCC patients between 20 IC genes and 6 EMT-related genes. In the heatmaps, red indicates positive correlation, blue indicates negative correlation, and the intensity reflects correlation strength; significance is indicated by *, **, and *** for $p < 0.05$, 0.01, and 0.001, respectively.

Spearman correlation analysis, which captures monotonic associations, confirmed negative correlations of most ICs with CDH1 and generally weak associations with CDH2, except for NT5E, which displayed strong positive correlations with CDH2, suggesting a link to mesenchymal features. Notably, LGALS9, TNFRSF18, and CD276 were positively associated with TWIST1, SNAIL, and SLUG, while CD28 correlated with SNAIL and SLUG. VSIR showed positive correlation with the four EMT transcription factors. NT5E showed strong positive correlations with CDH2, SNAIL, SLUG and ZEB1. LAG3 also showed a positive association with TWIST1 (Figure 4B).

Taken together, these analyses highlighted ICs closely associated with EMT. Considering both statistical associations and biological relevance, LAG3 and NT5E were selected for further validation. LAG3 was prioritised as it correlated with EMT markers and for its established clinical relevance. FDA-approved targeting of LAG3 with Relatlimab/Nivolumab has demonstrated improved progression-free survival and a favourable toxicity profile in advanced melanoma [35]. NT5E was selected based on its strong associations with mesenchymal markers and our previous demonstration that it is EMT-regulated [26].

 doi:10.20944/preprints202604.2137.v1

3.4. Co-Localisation of EMT and ICs in ccRCC Patients

To evaluate the relationship between EMT status and two IC genes, LAG3 and NT5E, single-cell transcriptomic data from seven ccRCC patients were analysed. Tumor cells were classified using the ccRCC.epi and ccRCC.mes signatures to distinguish epithelial and mesenchymal states. Uniform Manifold Approximation and Projection (UMAP) plots illustrate EMT-positive cells (Figure 5A), with epithelial and mesenchymal populations highlighted separately (Figure 5B, C). Across all patient samples, tumor cells exhibited co-expression of EMT markers and IC genes LAG3 (Figure 5D) and NT5E (Figure 5E), indicating that immune-related programs are active in both epithelial and mesenchymal tumor cells. A representative patient sample is presented in Figure 5, while a second patient sample displaying similar expression patterns is presented in Supplementary Figure S4.

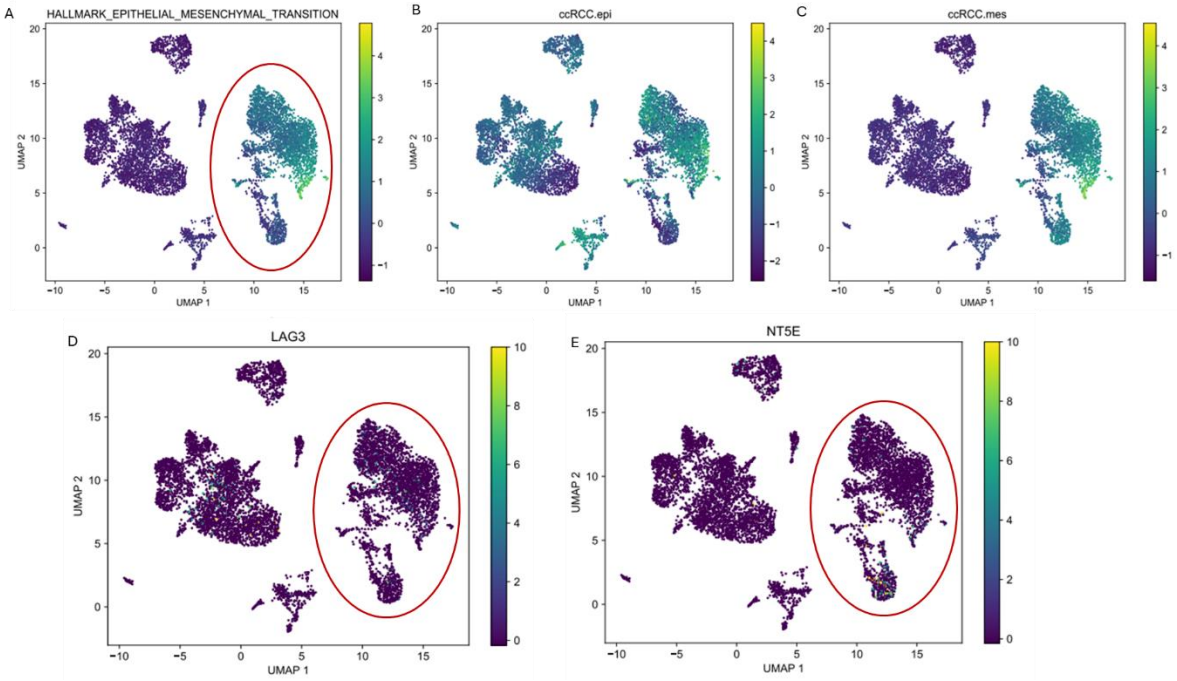

Figure 5. Single-cell co-localisation of EMT states and IC gene expression in ccRCC tumors. (A) UMAP plot showing EMT-positive tumor cells identified across ccRCC patients; a representative patient is shown. Red circle indicates EMT-positive cluster (B) Distribution of epithelial tumor cells classified using the ccRCC.epi signature. (C) Distribution of mesenchymal tumor cells classified using the ccRCC.mes signature. UMAP plot showing expression of (D) LAG3 and (E) NT5E across tumor cells. Red circle highlighted EMT-positive cluster co-expressing LAG3 or NT5E.

Additionally, other IC genes were also observed to align with EMT-positive cells across patient samples (Figure S5). Notably, expression of IC genes was not restricted to tumor cells but was also detected in multiple non-tumor cell types within the TME. These results highlight coordinated patterns of EMT and immunomodulatory gene expression at the single-cell level in ccRCC, supporting the concept of an EMT–IC axis.

Next, we performed immunohistochemistry to examine the localisation of the epithelial marker E-cadherin and the mesenchymal marker N-cadherin with LAG3 and NT5E (Figure 6 and 7). Across the three patient samples analysed, LAG3 and NT5E expression were observed in subsets of both E-cadherin-positive and N-cadherin-positive tumor cells. These findings indicate co-expression of LAG3 and NT5E with both epithelial and mesenchymal markers within the tumor further supporting the presence of an EMT–IC axis in ccRCC.

 doi:10.20944/preprints202604.2137.v1

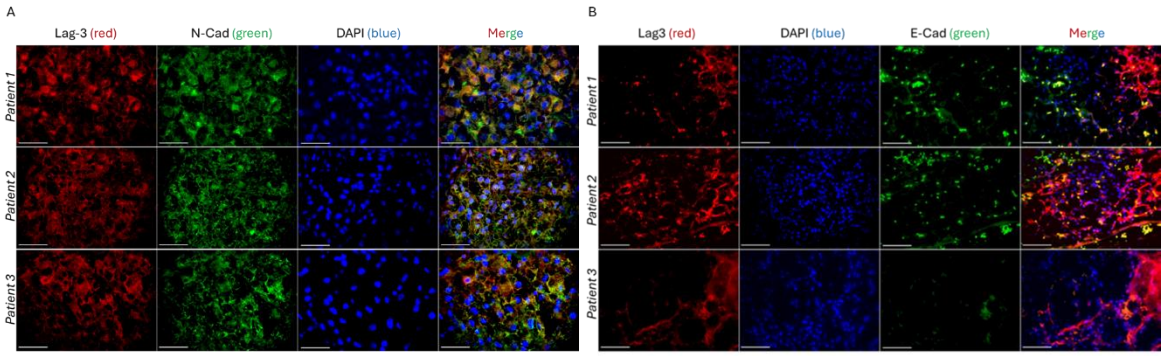

Figure 6. Localisation of LAG3 with epithelial and mesenchymal markers in ccRCC tumor tissues. Representative immunohistochemical staining of LAG3 (red) in combination with the mesenchymal marker N-cad (green) and the epithelial marker E-cad (green) in three ccRCC tumor samples. Nuclei were counterstained with DAPI (blue). Merged images showed the overlay of all three channels. Scale bar 100 μm.

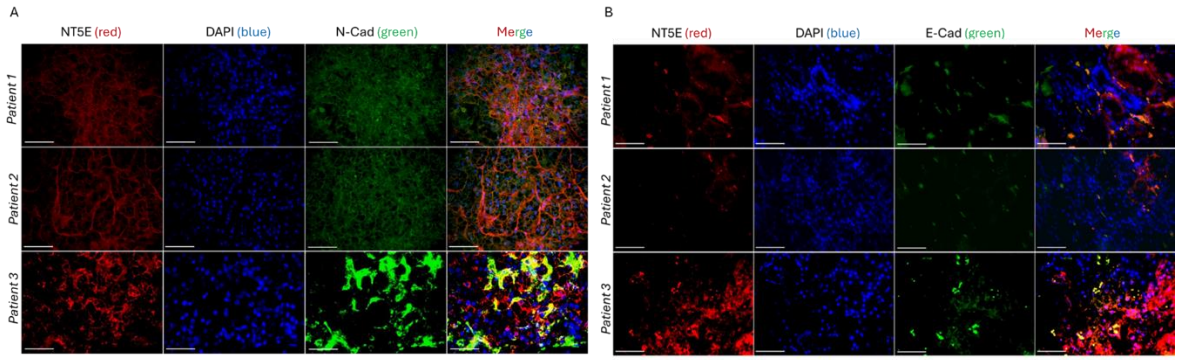

Figure 7. Localisation of NT5E with epithelial and mesenchymal markers in ccRCC tumor tissues. Representative immunohistochemical staining of NT5E (red) in combination with the mesenchymal marker N-cad (green) and the epithelial marker E-cad (green) in three ccRCC tumor samples. Nuclei were counterstained with DAPI (blue). Merged images showed the overlay of all three channels. Scale bar 100 μm.

3.5. Time-Dependent ROC Analysis of the EMT–IC Axis in ccRCC

ROC analysis was performed to evaluate the predictive performance of IC genes alone and in combination with EMT markers for overall survival in 415 ccRCC patients. Individually, both IC genes LAG3 and NT5E showed limited predictive ability, with AUC values remaining relatively stable over time. Individually, LAG3 showed AUC values remaining relatively stable over time, ranging from approximately 0.55 at 500 days to 0.59 at 4000 days (Figure 8A). In contrast, combining LAG3 with the six EMT markers substantially improved predictive performance. The combined model achieved an AUC of 0.73 at 500 days to 0.68 at 4000 days (Figure 8B). Similarly, NT5E alone showed AUC values ranging from 0.57 at 500 days to 0.66 at 4000 days. The combined EMT–NT5E model showed improved predictive accuracy overall, with AUC values ranging from 0.73 at 500 days to 0.68 at 4000 days. The combined models consistently outperformed IC genes alone across all time points, with the strongest prognostic performance observed at earlier time points. These findings further support the prognostic value of the EMT–IC axis in ccRCC.

 doi:10.20944/preprints202604.2137.v1

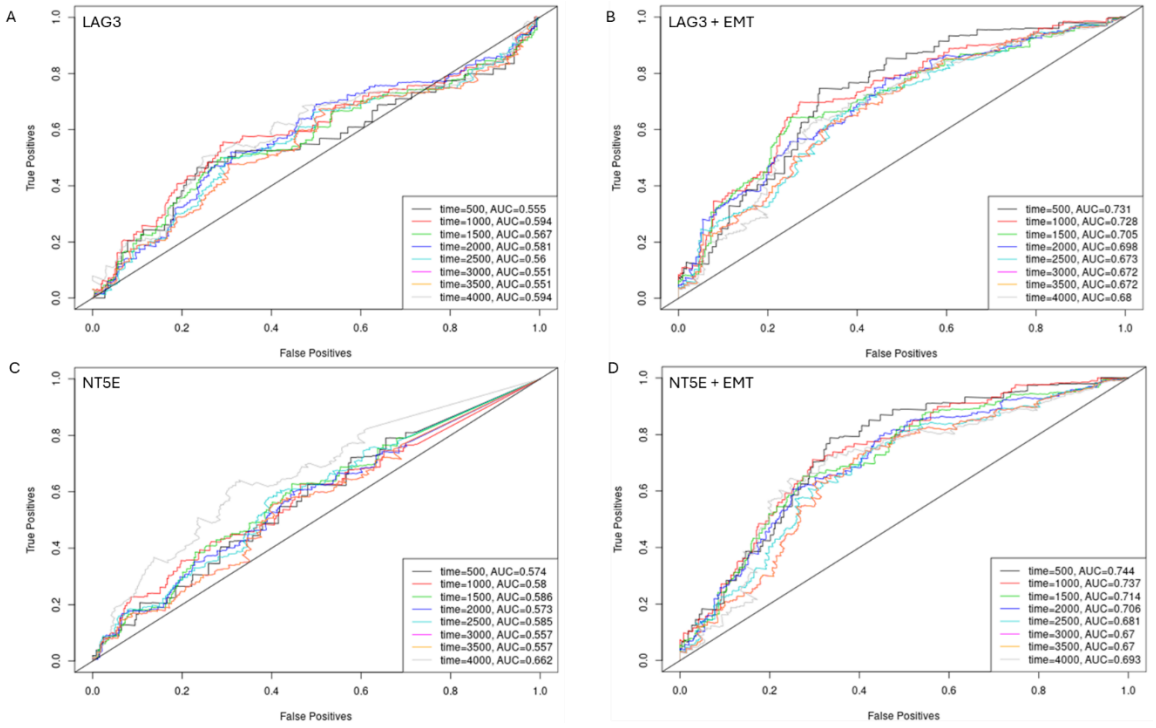

Figure 8. Time-dependent ROC analysis of IC genes alone and in combination with EMT markers for prediction of overall survival in ccRCC patients. Time-dependent ROC curves showing the predictive performance of (A) LAG3 alone, (B) the combined LAG3–EMT model, (C) NT5E alone, and (D) the combined NT5E–EMT model across time points ranging from 500 to 4000 days.

4. Discussion

In the present study, we explored the interplay between IC and EMT in ccRCC, defining a prognostically relevant EMT–IC axis. Central to this axis are LAG3 and NT5E, which emerged as promising prognostic biomarkers and potential therapeutic target through integrating single-cell and bulk transcriptomics, along with immunohistochemistry analyses. Notably, LAG3 and NT5E expression was strongly associated with poor overall survival and their combination with the EMT phenotype improved prognostic discrimination compared to individual ICs. ROC analyses further highlighted the potential clinical utility of LAG3 and NT5E.

ccRCC is a highly heterogeneous tumor, and robust biomarkers are urgently needed to improve prognostic determination and inform treatment decisions. Our findings, together with those of previous findings indicate IC expression and pathway dysregulation is a prominent feature of ccRCC [27]. Our analysis of 537 ccRCC patients versus 72 normal kidney samples revealed significant upregulation of 19 out of 20 ICs in ccRCC patient tumors. In contrast, a previous study which examined 534 patients and 15 IC genes, overlapped with five of the ICs we interrogated, namely, PD-L1, CTLA4, LAG3, HAVCR2 and CD276 [27]. PD-L1 showed discordant results between the studies, where PD-L1 differential expression did not reach significance in the previous study [27]. This discrepancy may reflect the small increase in patient numbers and differences in data preprocessing and analysis methods. Notably, our observation of an increase in multiple secreted IC proteins following Nivolumab monotherapy in a ccRCC patient who did not respond to therapy likely reflects adaptive resistance mechanisms. Given the dysregulation of several IC molecules in ccRCC patients, further exploration of alternative and complementary IC targets may provide additional opportunities for immunotherapeutic intervention in this cancer subtype.

PD-L1 (CD274), used as a routine IC biomarker in cancers such as melanoma and non-small cell lung cancer, has failed in its accuracy and specificity in predicting sensitiveness to immunotherapy and prognosis of ccRCC patients [36]. PD-L1 assessment is not clinically helpful in initiating therapy with ICI for patients with ccRCC. In line with this, PD-L1 expression was not significantly associated

 doi:10.20944/preprints202604.2137.v1

with poor prognosis in the ccRCC patient cohort analysed, despite being upregulated in ccRCC tumors relative to normal kidney tissues. Similarly, high PD-L1 expression was not associated with poor patient outcomes, while others have linked PD-L1 expression with poor outcomes in ccRCC patients [22,37]. This discrepancy may reflect heterogeneous expression of PD-L1 in patient TME [38].

CTLA4 is a transmembrane protein that negatively regulates T-cell activation through competitively blocking the binding of CD28 with B7, leading to immune evasion [39]. We and others have observed high CTLA4 expression was associated with poor overall survival in ccRCC patients [40–42]. Lymphocyte-activation gene 3 (LAG3 or CD223) negatively regulates T-cell activation and function. Similar to PD-1 blockers, blocking LAG3 activates effector T-cells [43]. Multiple LAG3 inhibitors are being currently evaluated in ccRCC patient clinical trials. Our finding that LAG3 expression is linked with poor ccRCC patient overall survival is consistent with a previous study [44]. These findings suggest that in addition to being administered for ccRCC patient treatment, these IC molecules can be beneficial for screening and selecting ccRCC patients who are at increased risk of worse survival.

NT5E is a glycophosphatidylinositol-anchored receptor enzyme that binds to adenosine to inhibit the T-cell activation [20]. Among 44 ccRCC cases, NT5E was more intensively expressed in high-grade G3 and G2 tumors indicating a link with tumor aggressiveness [45]. Similarly, our study shows marked elevation of NT5E expression in ccRCC tumors relative to normal kidney tissues. We also report on the prognostic association between ccRCC patient survival and NT5E expression. This is consistent with our observations in other solid cancers and a report from Zhou et al in ccRCC, supporting NT5E as a clinically relevant prognostic marker [19,20,46].

CD80 (B7-1) is a ligand recognised by CD28 resulting in T-cell activation. Consistent with our findings, Bao et al. reported that elevated expression of CD80 was associated with poor prognosis in ccRCC patients [47][46]. Glucocorticoid-induced tumor necrosis factor family receptor (GITR) or TNFRSF18 is an attractive target for immunotherapy due to its capacity to promote effector T-cell functions and hamper regulatory T-cell suppression [48][56]. We found that elevated levels of TNFRSF18 were a significant predictor of poor overall survival in ccRCC patients, consistent with findings from a previous study in ccRCC [49]. CD276, also known as B7 homologue 3 (B7-H3), functions as a T-cell inhibitor promoting tumor proliferation and invasion. CD276 expression in ccRCC tumor cells or within tumor vasculature was associated with an increased risk of death [50][45]. This is in line with our observation that high CD276 expression is associated with poor overall survival. LGALS9 or Galectin-9 is a member of the galectin family of animal lectins that binds to the HAVCR2 receptor to limit T-cell responses. We found elevated expression of LGALS9 was associated with poor overall survival, in line with a report highlighting a link with both survival and early recurrence in ccRCC patients [51]. CD27, a receptor for CD70, is correlated with worse survival in ccRCC patients who have CD27 positive lymphocyte tumor infiltration [52]. Our study similarly associated elevated CD27 expression with poor overall survival. TIGIT expression was also associated with poor ccRCC patient prognosis, in agreement with an earlier study [53]. Collectively, while these ICs have been previously reported, our integrated EMT-IC analysis highlights LAG3 and NT5E as central components of a prognostically relevant axis in ccRCC, suggesting that specific ICs may differentially influence outcomes and represent priority targets for therapeutic intervention.

We explored the coordinated expression of immune regulators with EMT to understand their combined impact on ccRCC prognosis. Notably, ICs assessed were strongly linked to EMT status and in combination prognosticated worse patient outcomes. The improved prognostic performance of combined IC–EMT models in ROC analyses, suggest that EMT contributes to shaping the immune landscape in ccRCC and EMT-IC axis can serve as prognostic biomarkers and potential therapeutic targets for ccRCC patients. A study reported that EMT signatures correlated closely with IC gene signatures and could influence clinical outcomes in ccRCC patients [27]. N-cad was the only EMT marker in our study that overlapped with the 23 core EMT genes evaluated [27]. Another study suggested that ccRCC patients with a mesenchymal status determined by the expression of E-cad, N-cad, Vimentin and Fibronectin may respond better to combination treatment with ICIs and anti-

 doi:10.20944/preprints202604.2137.v1

angiogenic therapy [28]. We have previously demonstrated that EMT and ICs bidirectionally influence each other to facilitate tumor aggressiveness [26,54,55]. EMT has been reported to modulate the TME and promote immune evasion, which may contribute to cancer progression [56,57].

Importantly, the co-expression of LAG3 or NT5E with both epithelial and mesenchymal markers in single cell RNA seq and immunohistochemistry analyses suggests that IC-related programs are active across multiple EMT states, rather than being confined to purely epithelial or mesenchymal tumor cells. Furthermore, increase in secreted LAG3 levels in a ccRCC patient with poor clinical response to PD-1 blockade supports the role of LAG3 as a compensatory IC. This highlights its potential as both a predictive biomarker of ICI resistance and a rational target for combinatorial therapies in ccRCC, particularly within EMT-like tumor cell populations. Collectively, these findings further support the presence of an EMT–IC axis in ccRCC and indicates that EMT and immune regulation may be closely linked during tumor progression.

A limitation of our study is that ICI therapy analyses were restricted to one ccRCC patient, limiting conclusion about therapy resistance. Further studies to validate the expression of these immune predictors in larger ccRCC patient cohorts treated with ICI therapies are warranted. Additional validation of our findings in prospective studies would be necessary. The ccRCC patient cohort was small in single-cell seq RNA and immunohistochemistry study, and functional validation of the EMT–IC axis is lacking. Whilst this study focused on IC expression in ccRCC tumor cells, a comprehensive investigation of the composition of immune cells and their association with IC expression will aid in predicting ICI responses. While our study identifies a prognostically relevant EMT–IC axis, further experimental and clinical studies are needed to confirm its role in immune evasion and therapeutic targeting

5. Conclusions

ccRCC is the most lethal type of urogenital tumor with an increasing mortality rate over several years. Accordingly, better therapies with durable responses are needed to treat ccRCC patients. ICI-based immunotherapies alone or in combination with TKIs show promise for the non-surgical treatment of ccRCC. We examined the association between IC expression and EMT status in ccRCC, defining an EMT–IC axis in which EMT-like tumor cells coordinate NT5E or LAG3 expression, improving prognostic stratification and highlighting these checkpoints as potential biomarkers and therapeutic targets.

Supplementary Materials: The following supporting information can be downloaded at: Preprints.org, Figure S1: The OncoPrint analysis showing alterations in gene expression of immune checkpoint molecules in ccRCC patients.; Figure S2: Multiplex analysis of soluble immune checkpoint proteins in plasma from a ccRCC patient before and after Nivolumab treatment; Figure S3: Additional representative single-cell co-localisation of EMT states and LAG3 or NT5E gene expression in ccRCC tumors; Figure S4: Single-cell co-localisation of EMT states and immune checkpoint gene expression in ccRCC tumors; Table S1: SurvExpress-based overall survival of 415 ccRCC patients.

Author Contributions: Conceptualization, A.J. and P.P.; methodology, A.P, F.N.A., R.S, S.S., M.K.J., A.R., A.J. and P.P.; software, A.J., A.P, F.N.A., R.S, S.S., M.K.J., S.R., A.R. and P.P.; validation, A.P., F.N.A., R.S., and A.J.; formal analysis, A.P., F.N.A., R.S., S.S., M.K.J., P.P. and A.J.; investigation, A.P, F.N.A., R.S, S.S., M.K.J., A.J. and P.P.; resources, A.J., P.P., G.K., A.P., F.N.A., M.K.J.,S.R., and R.S.; data curation, A.P., F.N.A., R.S., S.S., M.K.J., S.R., A.R., R.S., A.J., P.P.; writing—original draft preparation, A.P., F.N.A, R.S., S.S., M.K.J., A.J., P.P.; writing—review and editing, A.P., F.N.A., R.S., R.S., G.K., A.J.,P.P.; visualization, A.P., A.J.; supervision, A.J., P.P.; project administration, A.J., P.P.; funding acquisition, G.K. All authors have read and agreed to the published version of the manuscript.".

Funding: This research received no external funding.

 doi:10.20944/preprints202604.2137.v1

Institutional Review Board Statement: The study was conducted in accordance with the Declaration of Helsinki, and approved by the Institutional Review Board (or Ethics Committee) of the Grampians Health and St John of God Healthcare Human Research Ethics Committee (protocol code 69601.

Informed Consent Statement: Informed consent was obtained from all subjects involved in the study.

Data Availability Statement: The data presented in this study are available on request from the corresponding authors.

Acknowledgments: We acknowledge support provided by the team at Fiona Elsey Cancer Research Institute towards this research. MKJ and SS were supported by Param Hansa Philanthropies.

Conflicts of Interest: The authors declare no conflicts of interest.

Abbreviations

The following abbreviations are used in this manuscript:

AUC	Area under the curve
B7-H3	B7 homologue 3
BTLA	B- and T-Lymphocyte Attenuator
C-index	concordance index
ccRCC	Clear cell renal cell carcinoma
CD	Cluster of Differentiation
CTLA4	Cytotoxic T-lymphocyte-associated antigen 4
EMT	Epithelial-to-mesenchymal transition
FASLG	Fas Ligand
GITR	Glucocorticoid-induced tumor necrosis factor family receptor
HAVCR2	Hepatitis A Virus Cellular Receptor 2
HRs	Hazard ratios
ICs	Immune checkpoints
ICIs	Immune checkpoint inhibitors
IDO-1	Indoleamine 2,3-dioxygenase 1
KIRC	Kidney Renal Clear Cell Carcinoma
LAG3	Lymphocyte Activation Gene-3
mTOR	Mammalian target of rapamycin
NT5E	Ecto-5′-Nucleotidase
ORR	Overall response rate
PD-1	Programmed cell-Death 1
PD-L1	Programmed Death Ligand 1
RCC	Renal cell carcinoma
ROC	Receiver operating characteristic
scRNA-seq	Single-cell RNA Sequencing
TIGIT	T cell immunoreceptor with Ig and ITIM domains
TKI	Tyrosine kinase inhibitors
TME	Tumor microenvironment
TNFRSF	Tumor Necrosis Factor Receptor Superfamily Member
TPM	Transcripts per million
UMAP	Uniform Manifold Approximation and Projection
VEGF	Vascular endothelial growth factor
VHL	Von Hippel Lindau
VSIR	V-Set Immunoregulatory Receptor

References

1. Bray, F., et al., Global cancer statistics 2018: GLOBOCAN estimates of incidence and mortality worldwide for 36 cancers in 185 countries. CA Cancer J Clin, 2018. 68(6): p. 394-424.

 doi:10.20944/preprints202604.2137.v1

2. Sharma, R., et al., Determinants of resistance to VEGF-TKI and immune checkpoint inhibitors in metastatic renal cell carcinoma. J Exp Clin Cancer Res, 2021. 40(1): p. 186.
3. Ricketts, C.J., et al., The Cancer Genome Atlas Comprehensive Molecular Characterization of Renal Cell Carcinoma. Cell Rep, 2018. 23(1): p. 313-326.e5.
4. Jonasch, E., J. Gao, and W.K. Rathmell, Renal cell carcinoma. Bmj, 2014. 349: p. g4797.
5. Heng, D.Y., et al., Cytoreductive nephrectomy in patients with synchronous metastases from renal cell carcinoma: results from the International Metastatic Renal Cell Carcinoma Database Consortium. Eur Urol, 2014. 66(4): p. 704-10.
6. Scholtes, M.P., et al., Biomarker-Oriented Therapy in Bladder and Renal Cancer. Int J Mol Sci, 2021. 22(6).
7. Goyal, A., et al., Pseudotumours in chronic kidney disease: can diffusion-weighted MRI rule out malignancy. Eur J Radiol, 2013. 82(11): p. 1870-6.
8. Makhov, P., et al., Resistance to Systemic Therapies in Clear Cell Renal Cell Carcinoma: Mechanisms and Management Strategies. Mol Cancer Ther, 2018. 17(7): p. 1355-1364.
9. Barata, P.C. and B.I. Rini, Treatment of renal cell carcinoma: Current status and future directions. CA Cancer J Clin, 2017. 67(6): p. 507-524.
10. Rini, B.I., Temsirolimus, an inhibitor of mammalian target of rapamycin. Clin Cancer Res, 2008. 14(5): p. 1286-90.
11. Lee, C.S., et al., Novel antibodies targeting immune regulatory checkpoints for cancer therapy. Br J Clin Pharmacol, 2013. 76(2): p. 233-47.
12. Thompson, R.H., et al., PD-1 is expressed by tumor-infiltrating immune cells and is associated with poor outcome for patients with renal cell carcinoma. Clin Cancer Res, 2007. 13(6): p. 1757-61.
13. Leite, K.R., et al., PD-L1 expression in renal cell carcinoma clear cell type is related to unfavorable prognosis. Diagn Pathol, 2015. 10: p. 189.
14. Flippot, R., B. Escudier, and L. Albiges, Immune Checkpoint Inhibitors: Toward New Paradigms in Renal Cell Carcinoma. Drugs, 2018. 78(14): p. 1443-1457.
15. Topalian, S.L., et al., Safety, activity, and immune correlates of anti-PD-1 antibody in cancer. N Engl J Med, 2012. 366(26): p. 2443-54.
16. Motzer, R.J., et al., Nivolumab plus Ipilimumab versus Sunitinib in Advanced Renal-Cell Carcinoma. N Engl J Med, 2018. 378(14): p. 1277-1290.
17. Santoni, M., et al., Immunotherapy in renal cell carcinoma: latest evidence and clinical implications. Drugs Context, 2018. 7: p. 212528.
18. Burgers, F.H., et al., Immunological features of clear-cell renal-cell carcinoma and resistance to immune checkpoint inhibitors. Nat Rev Nephrol, 2025. 21(10): p. 687-701.
19. Shrestha, R., et al., Monitoring Immune Checkpoint Regulators as Predictive Biomarkers in Hepatocellular Carcinoma. Front Oncol, 2018. 8: p. 269.
20. Cao, L., et al., Prognostic Role of Immune Checkpoint Regulators in Cholangiocarcinoma: A Pilot Study. J Clin Med, 2021. 10(10).
21. Beckermann, K.E., D.B. Johnson, and J.A. Sosman, PD-1/PD-L1 blockade in renal cell cancer. Expert Rev Clin Immunol, 2017. 13(1): p. 77-84.
22. Möller, K., et al., Tumor cell PD-L1 expression is a strong predictor of unfavorable prognosis in immune checkpoint therapy-naive clear cell renal cell cancer. Int Urol Nephrol, 2021. 53(12): p. 2493-2503.
23. Taki, M., et al., Tumor Immune Microenvironment during Epithelial-Mesenchymal Transition. Clin Cancer Res, 2021. 27(17): p. 4669-4679.
24. Soundararajan, R., et al., Targeting the Interplay between Epithelial-to-Mesenchymal-Transition and the Immune System for Effective Immunotherapy. Cancers (Basel), 2019. 11(5).
25. Yang, J., et al., Guidelines and definitions for research on epithelial-mesenchymal transition. Nat Rev Mol Cell Biol, 2020. 21(6): p. 341-352.
26. Cao, L., et al., CD73 and PD-L1 as Potential Therapeutic Targets in Gallbladder Cancer. Int J Mol Sci, 2022. 23(3).

 doi:10.20944/preprints202604.2137.v1

27. Liang, J., et al., The Correlation Between the Immune and Epithelial-Mesenchymal Transition Signatures Suggests Potential Therapeutic Targets and Prognosis Prediction Approaches in Kidney Cancer. Sci Rep, 2018. 8(1): p. 6570.
28. Chen, Q., et al., Deep Learning-Based Classification of Epithelial-Mesenchymal Transition for Predicting Response to Therapy in Clear Cell Renal Cell Carcinoma. Front Oncol, 2021. 11: p. 782515.
29. Gao, J., et al., Integrative analysis of complex cancer genomics and clinical profiles using the cBioPortal. Sci Signal, 2013. 6(269): p. pl1.
30. Goldman, M.J., et al., Visualizing and interpreting cancer genomics data via the Xena platform. Nat Biotechnol, 2020. 38(6): p. 675-678.
31. Aguirre-Gamboa, R., et al., SurvExpress: an online biomarker validation tool and database for cancer gene expression data using survival analysis. PLoS One, 2013. 8(9): p. e74250.
32. Aibar, S., et al., SCENIC: single-cell regulatory network inference and clustering. Nat Methods, 2017. 14(11): p. 1083-1086.
33. Davidson, G., et al., Mesenchymal-like Tumor Cells and Myofibroblastic Cancer-Associated Fibroblasts Are Associated with Progression and Immunotherapy Response of Clear Cell Renal Cell Carcinoma. Cancer Res, 2023. 83(17): p. 2952-2969.
34. Prithviraj, P., et al., Aberrant pregnancy-associated plasma protein-A expression in breast cancers prognosticates clinical outcomes. Scientific Reports, 2020. 10(1): p. 13779.
35. Aggarwal, V., C.J. Workman, and D.A.A. Vignali, LAG-3 as the third checkpoint inhibitor. Nat Immunol, 2023. 24(9): p. 1415-1422.
36. Simonaggio, A., et al., Tumor Microenvironment Features as Predictive Biomarkers of Response to Immune Checkpoint Inhibitors (ICI) in Metastatic Clear Cell Renal Cell Carcinoma (mccRCC). Cancers (Basel), 2021. 13(2).
37. Stenzel, P.J., et al., Prognostic and Predictive Value of Tumor-infiltrating Leukocytes and of Immune Checkpoint Molecules PD1 and PDL1 in Clear Cell Renal Cell Carcinoma. Transl Oncol, 2020. 13(2): p. 336-345.
38. Jilaveanu, L.B., et al., PD-L1 Expression in Clear Cell Renal Cell Carcinoma: An Analysis of Nephrectomy and Sites of Metastases. J Cancer, 2014. 5(3): p. 166-72.
39. Gough, S.C., L.S. Walker, and D.M. Sansom, CTLA4 gene polymorphism and autoimmunity. Immunol Rev, 2005. 204: p. 102-15.
40. Klümper, N., et al., CTLA4 promoter hypomethylation is a negative prognostic biomarker at initial diagnosis but predicts response and favorable outcome to anti-PD-1 based immunotherapy in clear cell renal cell carcinoma. J Immunother Cancer, 2021. 9(8).
41. Liu, S., et al., CTLA4 has a profound impact on the landscape of tumor-infiltrating lymphocytes with a high prognosis value in clear cell renal cell carcinoma (ccRCC). Cancer Cell Int, 2020. 20: p. 519.
42. Xiao, G.F., et al., Identification of a Novel Immune-Related Prognostic Biomarker and Small-Molecule Drugs in Clear Cell Renal Cell Carcinoma (ccRCC) by a Merged Microarray-Acquired Dataset and TCGA Database. Front Genet, 2020. 11: p. 810.
43. Andrews, L.P., et al., LAG3 (CD223) as a cancer immunotherapy target. Immunol Rev, 2017. 276(1): p. 80-96.
44. Klümper, N., et al., LAG3 (LAG-3, CD223) DNA methylation correlates with LAG3 expression by tumor and immune cells, immune cell infiltration, and overall survival in clear cell renal cell carcinoma. J Immunother Cancer, 2020. 8(1).
45. Song, L., et al., Ecto-5'-nucleotidase (CD73) is a biomarker for clear cell renal carcinoma stem-like cells. Oncotarget, 2017. 8(19): p. 31977-31992.
46. Zhou, Y., et al., High expression of CD73 contributes to poor prognosis of clear-cell renal cell carcinoma by promoting cell proliferation and migration. Transl Cancer Res, 2022. 11(10): p. 3634-3644.
47. Bao, L., et al., The Identification of Key Gene Expression Signature and Biological Pathways in Metastatic Renal Cell Carcinoma. J Cancer, 2020. 11(7): p. 1712-1726.
48. Avogadri, F., et al., Modulation of CTLA-4 and GITR for cancer immunotherapy. Curr Top Microbiol Immunol, 2011. 344: p. 211-44.

 doi:10.20944/preprints202604.2137.v1

49. Liu, G., et al., Prognosis, Immune Microenvironment Infiltration and Immunotherapy Response in Clear Cell Renal Cell Carcinoma Based on Cuproptosis-related Immune Checkpoint Gene Signature. J Cancer, 2023. 14(17): p. 3335-3350.
50. Crispen, P.L., et al., Tumor cell and tumor vasculature expression of B7-H3 predict survival in clear cell renal cell carcinoma. Clin Cancer Res, 2008. 14(16): p. 5150-7.
51. Fu, H., et al., Galectin-9 predicts postoperative recurrence and survival of patients with clear-cell renal cell carcinoma. Tumour Biol, 2015. 36(8): p. 5791-9.
52. Ruf, M., H. Moch, and P. Schraml, Interaction of tumor cells with infiltrating lymphocytes via CD70 and CD27 in clear cell renal cell carcinoma. Oncoimmunology, 2015. 4(12): p. e1049805.
53. Yin, X., et al., Assessment for prognostic value of differentially expressed genes in immune microenvironment of clear cell renal cell carcinoma. Am J Transl Res, 2020. 12(9): p. 5416-5432.
54. Shrestha, R., et al., Immune checkpoint molecules are regulated by transforming growth factor (TGF)-β1-induced epithelial-to-mesenchymal transition in hepatocellular carcinoma. Int J Med Sci, 2021. 18(12): p. 2466-2479.
55. Shrestha, R., et al., Dual Targeting of Sorafenib-Resistant HCC-Derived Cancer Stem Cells. Curr Oncol, 2021. 28(3): p. 2150-2172.
56. Shrestha, R., et al., Combined Inhibition of TGF-β1-Induced EMT and PD-L1 Silencing Re-Sensitizes Hepatocellular Carcinoma to Sorafenib Treatment. J Clin Med, 2021. 10(9).
57. Poddar, A., et al., Crosstalk between Immune Checkpoint Modulators, Metabolic Reprogramming and Cellular Plasticity in Triple-Negative Breast Cancer. Curr Oncol, 2022. 29(10): p. 6847-6863.